

# Display Daylight Ambient Contrast Measurement Methods and Daylight Readability

**Edward F. Kelley,\***

National Institute of Standards and Technology, Boulder, Colorado, USA; kelley@nist.gov

**Max Lindfors, and**

Nokia, Helsinki, Finland; Max.Lindfors@nokia.com

**John Penczek**

DuPont Displays, Santa Barbara, California, USA; John.Penczek@usa.dupont.com

**Abstract:** *We propose two composite metrics to characterize display reflection, contrast, and readability under daylight illumination. A measurement of the reflection under directed illumination simulating the sun is combined with a measurement of the reflection under uniform diffuse illumination to simulate the sky. The measurements are performed separately in a laboratory, and then the measurement results are combined and scaled to daylight levels with attention to the proper spectra involved for the skylight and sunlight.*

**Key Words:** contrast; daylight readability; diffuse reflectance; directed source; display measurements; display readability; display reflection measurements; dynamic range; luminous reflectance factor; maximum readability; reflectance factor; skylight reflection; spectral reflectance factor; sunlight readability; sunlight reflection

## 1 Introduction

High demand exists for daylight-readable displays. At present the term “sunlight-readable” is ill-defined but commonly used. Often the display is placed outdoors in bright sunlight with the surrounding skylight to see whether it can be read easily. This is not objectionable, but it is not very reproducible. However, to simply point a spotlight with a sun-level illuminance at a display where the spotlight is placed at a substantial angle from the normal is *not* representative of daylight conditions. Such an arrangement neglects the contribution from a diffuse surround. We propose a general procedure to characterize

---

\*Optoelectronics Division, Electronics and Electrical Engineering Laboratory, Technology Administration, U.S. Department of Commerce.

This is a contribution of the National Institute of Standards and Technology and is not subject to copyright.

the dynamic range, contrast, and readability of a display under daylight conditions. Two methods are presented: (1) the fixed-sun daylight configuration and (2) the optimized-sun daylight configuration.

This paper is a preliminary attempt to document measurement standards for daylight testing of displays. As such, these methods may not be applicable to all displays and may be regarded as areas for further research. Additionally, there may be other apparatus configurations that are important to provide a full reflection characterization of a display. The material presented here can serve as a template for other apparatus used to determine daylight contrasts and readability. The techniques discussed in this paper are to be performed in the laboratory. Both uniform diffuse illumination (uniform over  $2\pi$  sr) and directed illumination from a discrete source are made *separately* and then the results are combined and scaled mathematically to approximate the reflection characteristics at daylight levels.

## 2 Daylight Sources

In this section we specify the daylight composition and component spectra as well as other spectra and associated quantities to be used in calculations. As used in this paper, daylight is a combination of blue skylight and direct sunlight. For skylight, we will scale the measurement results for a uniform diffuse illumination with an illuminance level of  $E_{\text{sky}} = 10^4$  lx. For direct sunlight we will scale the measurement results for directed illumination at an illuminance level of  $E_{\text{sun}} = 10^5$  lx. However, please note that different levels of illuminance may be appropriate for different applications. We propose that if no illuminance levels are quoted with the results then the above levels shall be assumed. If other levels of illuminance are used, then they must be included with the reported measurement result.

The spectra and correlated color temperatures (CCTs) of the light sources used is important when there is significant color in reflection from the display surface or if the display surface exhibits fluorescence. If the display is truly gray in its reflection properties for all conditions of its operation, then the source spectrum is not important. Of course, in making this statement, we are considering only the visible spectrum. Mathematically speaking, a truly gray screen means that the spectral reflectance factor for all modes of operation of the display and in any environment is a constant for all wavelengths:

$$R_{\text{gray}}(\lambda) = R_{\text{gray}} = \text{constant.} \quad (1)$$

In most cases this grayness approximation is not sufficient, such as for colored reflective displays, displays having coatings giving a color to the reflection as via antireflection coatings, reflection for white screens where the internal colored filters affect the reflection properties, etc.

For the  $E_{\text{sky}}$  illuminance we will use a skylight spectrum corresponding to a CCT of  $T_{\text{sky}} = 16\,500$  K and for the  $E_{\text{sun}}$  illuminance we will use a sunlight spectrum corresponding to a CCT of  $T_{\text{sun}} = 5500$  K. The high CCT for the sky is selected, in part, so that the combination of skylight and sunlight provides an average CCT of 6500 K, equivalent to an overcast sky:

$$\frac{E_{\text{sky}}T_{\text{sky}} + E_{\text{sun}}T_{\text{sun}}}{E_{\text{sky}} + E_{\text{sun}}} = 6500 \text{ K} . \quad (2)$$

The normalized skylight spectrum  $S_{\text{sky}}(\lambda)$ , sunlight spectrum  $S_{\text{sun}}(\lambda)$ , and cloudy-day spectrum  $S_{\text{over}}(\lambda)$  are shown in Fig. 1. They are defined by the daylight eigenfunctions as specified by the methods provided by the CIE (Commission Internationale de l'Eclairage [International Commission on Illumination]): [1, 2]

$$S_{\text{D}}(\lambda) = [S_0(\lambda) + M_{\text{D}}S_1(\lambda) + M'_{\text{D}}S_2(\lambda)]/N_{\text{D}}, \quad (3)$$

where “D” represents the illumination condition,  $N_{\text{D}}$  is an appropriate normalization factor, and  $M_{\text{D}}$  and  $M'_{\text{D}}$  are the daylight eigenvalues—all found in Table 1. Also shown in Fig. 1 are the spectra of a tungsten-halogen source at a CCT of 2856 K and a tungsten-halogen source with an added infrared (IR) blocking filter (heat absorbing KG-3) to reduce near IR and heating—it provides a CCT of 3380 K. The illumination conditions employed in this paper are: D = sky, for skylight; D = sun, for sunlight; D = over, for overcast sky; D = tung, for a 2856 K tungsten-halogen source; and D = THIRB, for a tungsten-halogen source using an infrared (IR) blocking filter (KG-3 heat absorbing filter). The units of the spectra  $S_{\text{D}}(\lambda)$  are set to be  $(\text{nm})^{-1}$  so that a wavelength integration is without units—accomplished by assigning the units of nm to the normalization  $N_{\text{D}}$ . Also included in the table are scaling factors  $f_{\text{D}}$  (unit:  $\text{W}/\text{m}^2$ ) that are needed in later calculations to obtain the required illuminances:

$$f_{\text{D}} K_{\text{m}} \int_{360 \text{ nm}}^{830 \text{ nm}} V(\lambda)S_{\text{D}}(\lambda)d\lambda = E_{\text{D}}, \quad (4)$$

where  $K_{\text{m}} = 683 \text{ lm}/\text{W}$  is the maximum luminous efficacy of radiation, and  $V(\lambda)$  is the spectral luminous efficiency of the human eye. Note that all wavelength integrations in this paper are assumed to be between 360 nm and 830 nm unless specified otherwise. Measurement results presented in this paper, however, are limited to the range 380 nm to 780 nm. We also define the integral as

$$G_{\text{D}} = \int V(\lambda)S_{\text{D}}(\lambda)d\lambda = \frac{E_{\text{D}}}{K_{\text{m}}f_{\text{D}}}, \quad (5)$$

where  $G_{\text{D}}$  is without units. The irradiances associated with the specified illuminances may be expressed as

$$E_{\text{D}}(\lambda) = f_{\text{D}} S_{\text{D}}(\lambda). \quad (6)$$

Note that in the determination of daylight reflection characteristics, the overcast sky and other illuminants are not employed as a surround condition to determine contrast or readability. They are included here for completeness and examples. Only  $S_{\text{sky}}(\lambda)$  and  $S_{\text{sun}}(\lambda)$  are used to determine daylight reflection characteristics.

Table 1. Daylight Eigenvalues and Spectral Factors					
Eigenvalues, Normalizations, Illuminances, and Scaling Factors (D = sky, sun, over, tung, THIRB)	Correlated Color Temperature (CCT)				
	16 500 K (D = sky)	6500 K (D = over)	5500 K (D = sun)	3380 K (D = THIRB)	2856 K (D = tung)
$M_D$	2.21902	-0.296340	-0.786338	—	—
$M'_D$	0.809706	-0.688321	-0.195381	—	—
$N_D$ (nm)	207.1359	117.7666	104.1987	—	—
$G_D = \int S_D(\lambda)V(\lambda)d\lambda$	53.91	89.73	100.87	86.80	48.42
$E_D = E_{\text{sun}}, E_{\text{over}}, E_{\text{sky}}$ (lx)	10 000	Heavy: 1000 Light: 10 000	100 000	—	—
$f_D = f_{\text{sun}}, f_{\text{over}}, f_{\text{sky}}$ (W/m <sup>2</sup> )	0.2716	0.01632	1.452	—	—

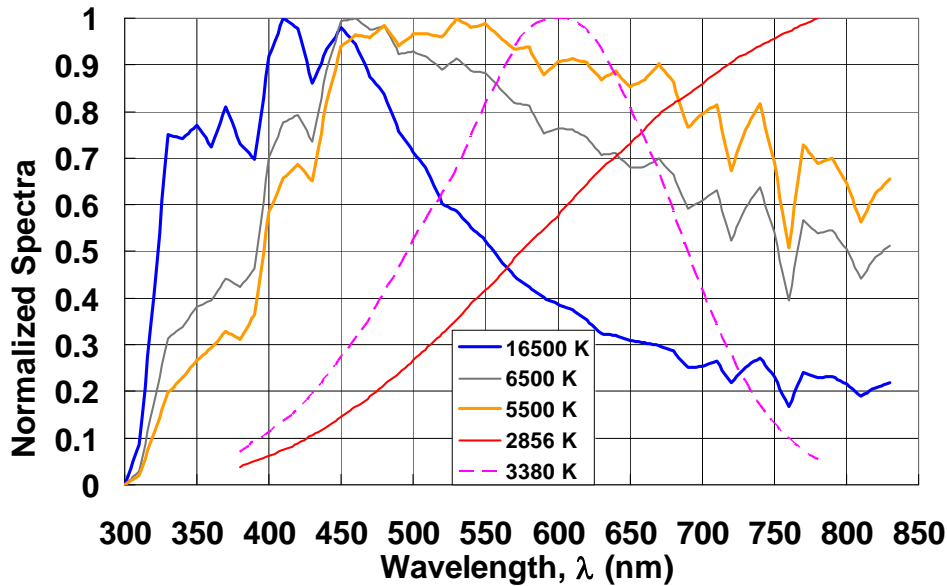


**Figure 1.** Spectra for skylight at 16 500 K,  $S_{\text{sky}}(\lambda)$ , sunlight at 5500 K,  $S_{\text{sun}}(\lambda)$ , and overcast daylight at 6500 K,  $S_{\text{over}}(\lambda)$ . These spectra are calculated by the CIE-15 method. Laboratory sources at 2856 K,  $S_{\text{tung}}(\lambda)$ , and 3380 K,  $S_{\text{THIRB}}(\lambda)$ , are included.

Laboratory tungsten-halogen sources can often be converted to these CCTs by means of various combinations of colored filters, e.g., photographic color-conversion filters 80A, 80B, 80C, 80D, or light-balancing filters 82, 82A, 82B, 82C, or other types of correcting filtration. Figure 2 shows how a tungsten-halogen illuminant with a CCT of 2856 K can be filtered to obtain CCTs of 5500 K, 6500 K, and 16 500 K illumination. Such attempts to filter tungsten-halogen sources to obtain daylight spectra do maintain the broadband nature of the daylight sources, but they are only crude approximations to the daylight spectra. Because of manufacturing inconsistencies, age, and temperature, no definite prescriptions can be offered for accurate conversions. It is necessary to measure just how the combinations affect the illumination to give the proper CCT. If

there is any nontrivial fluorescence in the display components, then the correct broadband illumination spectrum may be needed or the spectral fluorescence characteristics may need to be determined and properly handled.

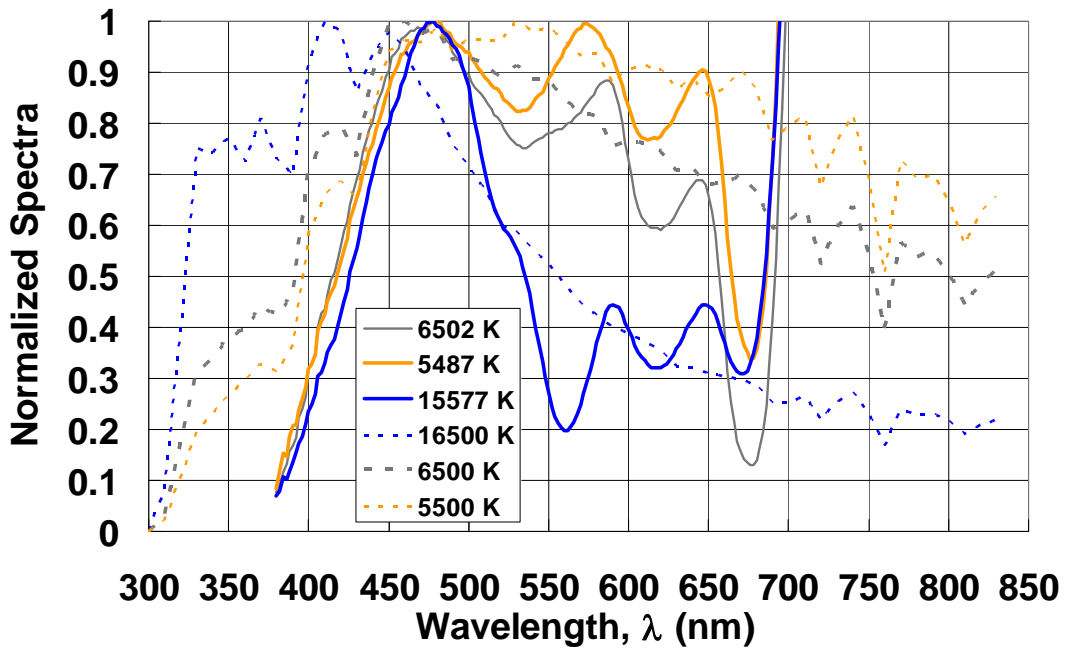


**Figure 2.** Approximate daylight and sunlight spectra by use of photographic color-correction filters graphed in solid lines. Data are normalized over 350 nm to 650 nm. The dashed lines represent the target spectra for the 16500 K skylight spectrum  $S_{\text{sky}}(\lambda)$ , the 5500 K sunlight spectrum  $S_{\text{sun}}(\lambda)$ , and the 6500 K overcast-day spectrum  $S_{\text{over}}(\lambda)$ . In the region beyond 700 nm the filtered spectra reach the maximum value of approximately 6.5 on this scale at 780 nm (our limit of measurement).

Because of the limitations in using filters to attempt to accurately correct for the proper CCTs, we suggest that spectral reflection measurements be made and then the appropriate reflection parameter be determined based upon the ideal spectral illuminants given in Eqs. (3) and (4) and illustrated in Fig. 1. Although the required detector is a spectroradiometer or equivalent in order to obtain these results, the required lighting apparatus is much more easily obtained because a specific source spectral content is not required. The extra cost for the detector is traded for the lower cost of the sources. It will be shown below that the reflected light from the display must be significantly brighter than any self-luminance from an emissive display in order to reduce the uncertainty in the measurement results. Attempting to provide filtration of normal laboratory sources can greatly reduce their brightness making them less suitable for reflection measurements with emissive displays.

### 3 Spectral Reflection Measurement Theory

In what follows, we will depart somewhat from the conventional notation for radiometric and photometric quantities. We will express all radiometric quantities, such as radiance  $L(\lambda)$ , and other wavelength-dependent quantities, such as spectral diffuse reflectance  $\rho(\lambda)$ , by explicitly showing their wavelength dependence. Reflection parameters, such as diffuse

reflectance  $\rho$  and luminance factor  $\beta$ , or the photometric quantities, such as luminance  $L$  and illuminance  $E$ , will *not* have a wavelength dependence explicitly shown. Often in the literature a subscript “ $\lambda$ ” or “ $e$ ” is used for radiometric quantities and a subscript “ $v$ ” is used for photometric quantities whenever both radiometric and photometric quantities are under discussion. We will depart from this subscript convention to avoid complicated subscripts and depend only upon an explicit wavelength dependence “ $(\lambda)$ ” to identify the radiometric quantities.

The spectral reflectance factor  $R(\lambda)$  is the ratio of the reflected spectral radiance of the display surface to the reflected spectral radiance of a perfect reflecting diffuser subjected to the same illumination conditions (measurement geometry and spectra) where the detector cone of acceptance is defined. Using the reflectance factor as well as any other reflection parameter requires that the geometry of the measurement apparatus be specified completely including illumination and viewing angles. This means that the detector geometry (acceptance area, distance, etc.) and the source geometry (size, distance, etc.) are completely specified. For the purposes of this paper, we are assuming unpolarized illumination.

Often in the display industry, the detector angular aperture (acceptance area subtense) is not an important factor unless it is too large as when the detector is placed too close to the display—closer than the eye would normally be placed. When we assume that the detector acceptance area is essentially zero or ignorable, we can use the quantity spectral radiance factor  $\beta(\lambda)$ , which is the same as the spectral reflectance factor but assuming a detector with no solid-angle subtense for its acceptance area, that is, having zero angular aperture—a point detector. Another reflection parameter of interest is the spectral diffuse reflectance  $\rho(\lambda)$  defined as the ratio of the diffusely reflected radiant flux to the incident radiant flux. Often it is measured by subjecting the surface to a beam of light at a certain angle  $\theta$  from the normal of the sample and measuring the reflected total radiant flux diffusely—often expressed as  $\rho_{\theta d}(\lambda)$ . Because light can travel in either direction (Helmholtz reciprocity)  $\rho_{\theta d}(\lambda)$  is equivalent to  $\beta_{d/\theta}(\lambda)$  where the detector is placed at an angle  $\theta$  from the normal and the surface is illuminated with uniform diffuse illumination. For all these reflection parameters ( $R$ ,  $r$ ,  $b$ ) we will use a subscript “ $H$ ” to denote the color of the display. In this paper  $H = W$  for white screens and  $H = K$  for black screens.

The photometric reflection parameters are obtained by using radiometric quantities that are integrated against the spectral luminous efficiency  $V(\lambda)$  of the human eye. For example, the luminance is given in terms of the spectral radiance by

$$L = K_m \int L(\lambda)V(\lambda) d\lambda , \quad (7)$$

where  $K_m = 683 \text{ lm/W}$ . A similar expression can be written for the illuminance  $E$ . The reflection parameters are obtained from photometric quantities:  $R$  is the luminous reflectance factor; [3]  $\beta$  is the luminance factor; and  $\rho$  is the diffuse reflectance. The photometric reflection parameters ( $R$ ,  $\beta$ ,  $\rho$ ) are derived from the measured luminances and illuminances and are

not simply integrations of their spectrally resolved counterparts weighted by  $V(\lambda)$ . For example, the luminous reflectance factor  $R_H$  is written in terms of the spectral reflectance factor  $R_H(\lambda)$  as

$$R_H = \frac{\int V(\lambda)R_H(\lambda)E(\lambda)d\lambda}{\int V(\lambda)E(\lambda)d\lambda}, \quad (8)$$

for any given irradiance  $E(\lambda)$ , where the denominator is simply proportional (by  $K_m$ ) to the illuminance  $E$ . In what follows below, for clarity, we will use the luminance factor  $\beta$  in connection with discrete or directed sources and the diffuse reflectance  $\rho$  in connection with uniform diffuse illumination, rather than employ complicated subscripts with the reflectance factor. [4, 5, 6, 7, 8]

Suppose the display is exposed to a source of illumination that produces a measurable reflection in addition to any light emission from the display. Let  $E(\lambda)$  be the irradiance falling upon the display; such irradiance can include the back reflections from an emissive display as when placed in an integrating sphere as well as the irradiance arising from the lamp and its configuration. The spectral radiance measured in a darkroom with the display showing color H is  $L_H(\lambda)$ . When subjected to the illumination producing reflection the spectral radiance becomes  $L(\lambda)$ . The spectral reflectance factor is given by

$$R_H(\lambda) = \frac{\pi[L(\lambda) - L_H(\lambda)]}{E(\lambda)}, \quad (9)$$

where the quantity in brackets is the net reflected spectral radiance. The radiances in the darkroom and under illumination must be measured at the same angle from the normal of the display (screens can exhibit a strong viewing-angle dependence), at the same position on the display surface (screens can be very nonuniform), and as close to the same time as possible (screens can vary in time). Note that for any apparatus configuration we always want to arrange for sufficient irradiance so that the reflected spectral radiance  $L(\lambda) - L_H(\lambda)$  is adequately measurable compared to the intrinsic darkroom spectral radiance  $L_H(\lambda)$  of the display for any color being displayed; otherwise the difference in the numerator above will be small and the measurement result may exhibit a large uncertainty. We must also be careful not to heat the display by the source because some displays exhibit a nontrivial temperature dependence.

If an irradiance meter is not available for measuring the irradiance  $E(\lambda)$ , we can attempt to measure the irradiance by using a white standard that has been calibrated for that illumination geometry. Note that the white standard *must* be calibrated for the illumination geometry employed; it is not correct to simply use a diffuse-reflectance value of, say, 0.99 for all illumi-

nation geometries. For example, given the spectral reflectance factor  $R_{\text{std}}(\lambda)$  of the white standard for the illumination geometry under consideration, the spectral irradiance  $E(\lambda)$  can be obtained from the spectral radiance  $L_{\text{std}}(\lambda)$  of the standard:

$$E(\lambda) = \frac{\pi L_{\text{std}}(\lambda)}{R_{\text{std}}(\lambda)}. \quad (10)$$

For such a situation, the spectral reflectance factor is given in terms of spectral radiance measurements only:

$$R_{\text{H}}(\lambda) = \frac{R_{\text{std}}(\lambda)[L(\lambda) - L_{\text{H}}(\lambda)]}{L_{\text{std}}(\lambda)}. \quad (11)$$

In the rare event that a special need arises to filter the light reaching the detector, a filter may be placed in front of the detector provided that all the radiances in Eq. (11) are measured through the same filter—this would include the darkroom measurements of the display. For such a case, the spectral transmittance  $\tau(\lambda)$  of the filter becomes a product of all the radiances and divides out—only the measurement suggested by Eq. (11) may be used for this. However, if we are *not* making spectrally resolved radiometric measurements, we cannot, in general, place a filter in front of the detector to determine the reflection parameters.

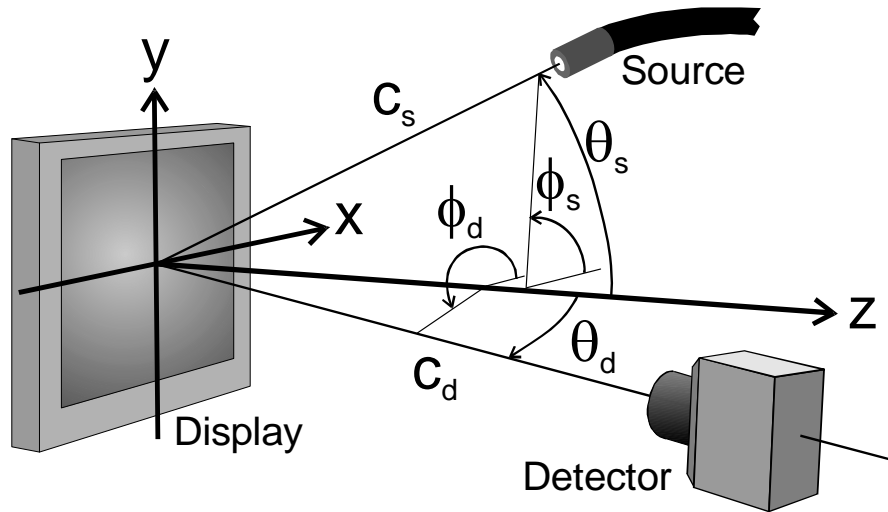


**Figure 3.** Coordinate system with a directed source with center at angles  $(\theta_s, \phi_s)$  and detector at  $(\theta_d, \phi_d)$ . For a replication of the sun, the source diameter would subtend  $0.5^\circ$  as measured from the center of the screen.

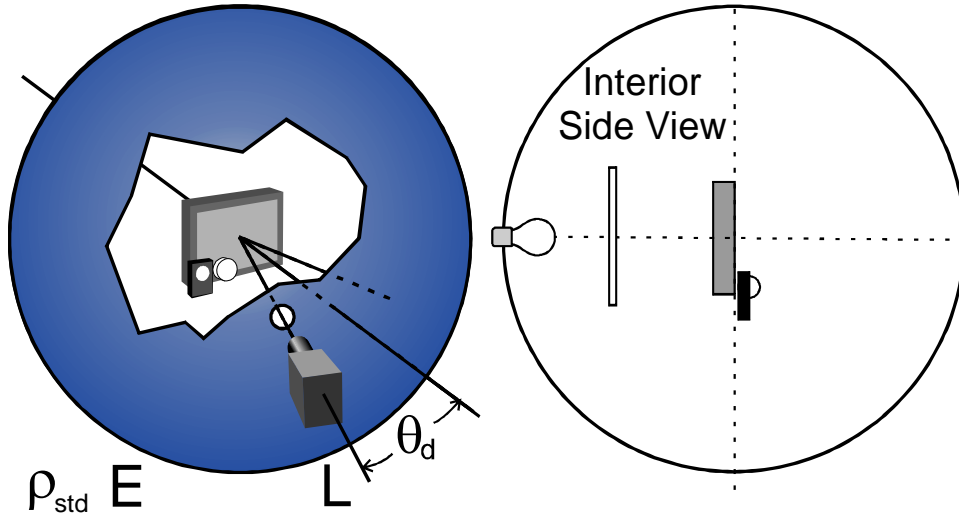


**Figure 4.** Diffuse-reflectance measurement with detector at angle  $\theta_d$  from the normal (from  $8^\circ$  to  $12^\circ$ ); configuration shown is for  $\phi_d = 180^\circ$ . White standard and irradiance meter are in place so all measurements are made without changing anything in the interior of the integrating sphere.

Two separate illuminating geometries are employed in making daylight reflection measurements. One uses a single directed source to simulate the sun and the other uses a uniformly diffuse source to simulate the sky. In general, these illumination geometries cannot be combined into one apparatus such as providing the directed source inside an integrating sphere—these require separate apparatuses providing separate measurement results.

The Cartesian coordinate system relative to the center of the screen is shown in Fig. 3 with spherical-polar coordinates locating the source  $(\theta_s, \phi_s)$  and detector  $(\theta_d, \phi_d)$ . The distance to the center of the source is  $c_s$ , and to the center of the detector is  $c_d$ . Figure 3 shows a directed source—a discrete source. Figure 4 shows a uniformly diffuse source as provided by the display being placed inside an integrating sphere. There are other configurations that may be used to provide a uniform diffuse illumination such as a sampling sphere. Using the directed source, we make a measurement of the spectral radiance factor  $\beta_H(\lambda; \theta_s, \phi_s, \theta_d, \phi_d)$ , and using the uniform diffuse illumination we make a measurement of the spectral diffuse reflectance  $\rho_H(\lambda; \text{diffuse}; \theta_d, \phi_d)$ .

### 3.1 Spectral Diffuse Reflectance

For the spectral diffuse reflectance measurement, we select the detector angle to be  $\theta_d = 10^\circ$  and  $\phi_d = 180^\circ$ . The spectral diffuse reflectance for uniform diffuse illumination is

$$\rho_H(\lambda) \equiv \rho_H(\lambda; \text{diffuse}; \theta_d=10^\circ, \phi_d=180^\circ). \quad (12)$$

We measure the spectral radiance of the screen under darkroom conditions

$$L_{Hu}(\lambda) \equiv L_{Hu}(\lambda; \theta_d=10^\circ, \phi_d=180^\circ), \quad (13)$$

obtaining  $L_{Wu}(\lambda)$  for the white screen and  $L_{Ku}(\lambda)$  for the black screen. The darkroom measurement is made from the same angle and at the same place on the screen as measured under uniform diffuse illumination. Here, the subscript “u” denotes uniform illumination. Under uniform illumination, the spectral radiance  $L_{hu}(\lambda)$  is measured for the white screen, and  $L_{du}(\lambda)$ , for the black screen (“h” is for high, “d” is for dark):

$$L_{hu}(\lambda) \equiv L_{hu}(\lambda; \theta_d=10^\circ, \phi_d=180^\circ), \quad (14)$$

and

$$L_{du}(\lambda) \equiv L_{du}(\lambda; \theta_d=10^\circ, \phi_d=180^\circ). \quad (15)$$

Because a display can modify the irradiance inside the sphere depending upon what it displays, associated with the spectral radiances are spectral irradiances  $E_h(\lambda)$  for the white screen and  $E_d(\lambda)$  for the black screen. However, having a bright integrating-sphere interior assures that any additions an emissive display makes to the irradiance will be small compared to the irradiance supplied by the integrating sphere. As generalized in Eq. (9), the spectral diffuse reflectances are given by

$$\begin{aligned} \rho_W(\lambda) &= \frac{\pi[L_{hu}(\lambda) - L_{Wu}(\lambda)]}{E_h(\lambda)} \\ \rho_K(\lambda) &= \frac{\pi[L_{du}(\lambda) - L_{Ku}(\lambda)]}{E_d(\lambda)}, \end{aligned} \quad (16)$$

where the numerators are the net reflected radiances. For many displays the diffuse reflectance exhibits little deviation over a detector angle range of  $6^\circ \leq \theta_d \leq 20^\circ$ ; so that the exact detector angle employed may not be critical. The diffuse measurement result will be included with any daylight reflection measurement.

It is important to note that the irradiance (or illuminance) must be measured with the display in place. Nothing can change inside the integrating sphere during all measurements except what is displayed on the screen. The interior geometry must be static for all measurements; this assures that any reflected radiance (luminance) contributing to the measurement of screen radiance (luminance) is directly related to the measured irradiance (illuminance).

### 3.2 Spectral Radiance Factor

Consider a small directed source that might simulate the subtense  $\kappa_s$  of the sun ( $0.5^\circ$ )—that is,  $\kappa_s = 0.5^\circ$ —placed at an arbitrary orientation  $(\theta_s, \phi_s)$ . Further, suppose we observe the display from another orientation  $(\theta_d, \phi_d)$ . In order to measure the spectral radiance factor

$$\beta_H(\lambda) \equiv \beta_H(\lambda; \kappa_s = 0.5^\circ; \theta_s, \phi_s, \theta_d, \phi_d) \quad (17)$$

for that configuration, we need to measure the darkroom luminances of the screen,

$$L_H(\lambda) \equiv L_H(\lambda; \theta_s, \phi_s, \theta_d, \phi_d) \quad (18)$$

at the same place and angle to be used when measured under illumination. Then we must measure the display under illumination:

$$L_h(\lambda) \equiv L_h(\lambda; \theta_s, \phi_s, \theta_d, \phi_d) \quad (19)$$

and

$$L_d(\lambda) \equiv L_d(\lambda; \theta_s, \phi_s, \theta_d, \phi_d), \quad (20)$$

where  $L_h(\lambda)$  is for the white screen and  $L_d(\lambda)$ , the black. The spectral radiance factors for the directed source are

$$\beta_W(\lambda) = \frac{\pi[L_h(\lambda) - L_W(\lambda)]}{E(\lambda)} \quad (21)$$

and

$$\beta_K(\lambda) = \frac{\pi[L_d(\lambda) - L_K(\lambda)]}{E(\lambda)},$$

where it is assumed that the display color has no effect upon the spectral irradiance  $E(\lambda)$ —generally the directed source is very bright and is not influenced by any outside conditions. This kind of measurement simulates how a hand-held display can be oriented relative to the sun in order to maximize the contrast or readability. The requirement that the source have the same subtense as the sun ( $\kappa_s = 0.5^\circ$ ) renders the measurement result more robust. However, depending upon the reflection properties of the display, this subtense requirement may be relaxed somewhat, permitting a subtense of up to a few degrees. This matter will be discussed further in the section describing the configurations below.

### 3.3 Darkroom Radiances in Design Viewing Direction

Associated with any display is a design viewing direction  $(\theta_d', \phi_d')$ . For most displays this is the normal direction ( $\theta_d' = 0, \phi_d' = 0$ ). Darkroom measurements on emissive displays provide the radiance for the displayed color H in the design viewing direction denoted by

$$J_H(\lambda) = J_H(\lambda; \theta_d', \phi_d'). \quad (22)$$

To the darkroom spectral radiances  $J_W(\lambda)$  and  $J_K(\lambda)$  will be added the daylight net reflected spectral radiances that are calculated based upon the daylight spectral irradiances and measured spectral reflection parameters. The spectral radiances  $L_H(\lambda)$  and  $J_H(\lambda)$  can differ, especially for the diffuse measurement, in that  $L_H(\lambda)$  is measured from the same direction as used for the reflection measurement, whereas  $J_H(\lambda)$  is measured from the design viewing direction (often the normal direction). For example, in the diffuse measurement  $L_H(\lambda)$  is measured at  $10^\circ$  from the normal, but  $J_H(\lambda)$  may be measured from along the normal.

### 3.4 General Daylight Calculations

We combine the spectral diffuse reflectance measurement and the spectral radiance measurement to calculate the observed spectral radiance  $K_H(\lambda)$  under daylight conditions—a composite metric to characterize daylight performance:

$$K_H(\lambda) = J_H(\lambda) + \frac{\rho_H(\lambda)}{\pi} E_{\text{sky}}(\lambda) + \frac{\beta_H(\lambda)}{\pi} E_{\text{sun}}(\lambda) \cos \theta_s, \quad (23)$$

which gives us the white screen spectral radiance  $K_W(\lambda)$  and the black screen spectral radiance  $K_K(\lambda)$ . The first term is the contribution from the emissive display from the design viewing direction, the second term is the reflected radiance arising from the blue sky, and the third term is the reflected radiance arising from the direct sunlight at angle  $\theta_s$  relative to the screen normal. The resulting luminances become

$$K_H = J_H + \frac{K_m}{\pi} \int V(\lambda) \rho_H(\lambda) E_{\text{sky}}(\lambda) d\lambda + \frac{K_m \cos \theta_s}{\pi} \int V(\lambda) \beta_H(\lambda) E_{\text{sun}}(\lambda) d\lambda, \quad (24)$$

where the  $J_H$  are the darkroom luminances at the design viewing direction, and the other two terms provide the luminance contributions of the skylight and the sunlight. In photopic quantities, this is

$$K_H = J_H + \frac{\rho_H}{\pi} E_{\text{sky}} + \frac{\beta_H}{\pi} E_{\text{sun}} \cos \theta_s, \quad (25)$$

for  $H = W$  for the white screen and  $H = K$  for black.

At this point we define an ambient dynamic range, ambient contrast ratio, or full-screen contrast ratio under specified ambient conditions as [9]

$$D = K_W/K_K. \quad (26)$$

Related to such a dynamic range or full-screen contrast ratio is another contrast metric with a maximum of one and a minimum of zero:

$$C \equiv (L_{\text{max}} - L_{\text{min}})/L_{\text{max}} = (K_W - K_K)/K_W = (D - 1)/D. \quad (27)$$

However, note that readability is not dependent only upon contrast; more is needed, and this situation is covered below in section 7.

## 4 Measurement Configurations

There are two configurations that we propose to represent proper daylight characterizations of displays: (1) fixed-sun daylight configuration, and (2) optimized-sun daylight configuration. For these configurations a diffuse skylight is combined with directed sunlight to provide spectral radiance levels for white and black screens,  $K_w(\lambda)$  and  $K_k(\lambda)$ , respectively.

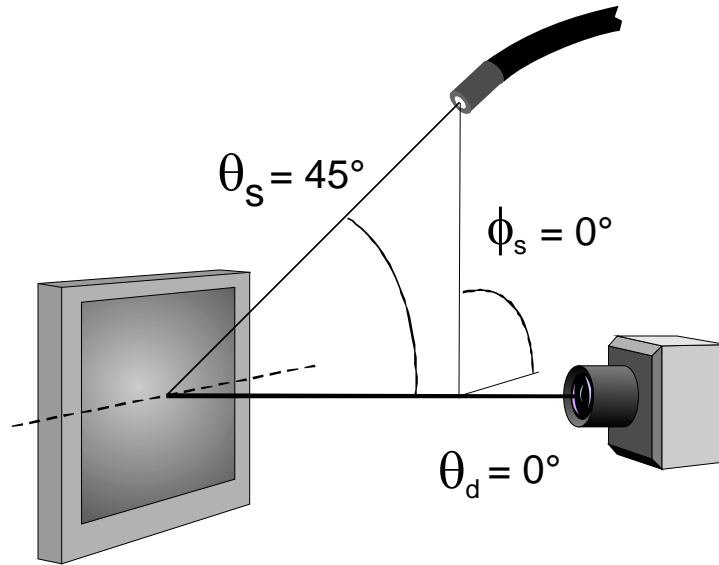


**Figure 5.** Fixed-sun configuration with source at  $45^\circ$  above the normal and the detector on the normal.

### 4.1 Fixed-Sun Daylight Configuration

The fixed-sun configuration assumes that the sun is at  $45^\circ$  overhead behind the user—see Fig. 5. The detector is positioned in the design viewing direction  $\theta_d'$ ,  $\phi_d'$ . The small directed source is placed at the direction  $\theta_s = 45^\circ$ ,  $\phi_s = 90^\circ$ . Ideally, the source should have a subtense of  $0.5^\circ$  simulating the angular size of the sun,  $\kappa_s = 0.5^\circ$ . We will use primes to denote this configuration. The spectral radiance factor is

$$\beta_H'(\lambda) \equiv \beta_H'(\lambda; \kappa_s = 0.5^\circ; \theta_s = 45^\circ, \phi_s = 90^\circ, \theta_d', \phi_d'). \quad (28)$$

The darkroom spectral radiances are

$$L_H'(\lambda) \equiv L_H'(\lambda; \theta_s = 45^\circ, \phi_s = 90^\circ, \theta_d', \phi_d'), \quad (29)$$

and the measured spectral radiances under illumination are measured at the same location on the screen,

$$L_h'(\lambda) \equiv L_h'(\lambda; \theta_s = 45^\circ, \phi_s = 90^\circ, \theta_d', \phi_d'), \quad (30)$$

$$L_d'(\lambda) \equiv L_d'(\lambda; \theta_s = 45^\circ, \phi_s = 90^\circ, \theta_d', \phi_d') \quad (31)$$

( $L_h'$  for white,  $L_d'$  for black). The spectral radiance factors for the fixed-sun source can then be calculated:

and

$$\beta_W'(\lambda) = \frac{\pi[L_h'(\lambda) - L_W'(\lambda)]}{E'(\lambda)} \quad (32)$$

$$\beta_K'(\lambda) = \frac{\pi[L_d'(\lambda) - L_K'(\lambda)]}{E'(\lambda)} ,$$

where it is assumed that the display color has no effect upon the irradiance  $E'(\lambda)$ . The spectral radiance under daylight conditions is determined by

$$K_H'(\lambda) = J_H(\lambda) + \frac{\rho_H(\lambda)}{\pi} E_{\text{sky}}(\lambda) + \frac{\beta_H'(\lambda)}{\pi} E_{\text{sun}}(\lambda) \cos \theta_s . \quad (33)$$

The white screen spectral radiance  $K_W'(\lambda)$  and the black screen spectral radiance  $K_K'(\lambda)$  provide the luminances  $K_W'$  and  $K_K'$  via Eq. (24). The ambient contrast ratio or dynamic range under daylight conditions is

$$D' = K_W'/K_K' \quad (34)$$

for the fixed-sun daylight configuration. Because the radiance-factor data are obtained from the source positioned at  $\theta_s=45^\circ$ , the measurement is somewhat robust even for a screen exhibiting a strong haze component of reflection. Although a source subtense of  $0.5^\circ$  is desired, it can sometimes be very difficult to arrange for a source sufficiently bright to give a reliable measurement of the reflected radiance (luminance). We have used sources with a subtense beyond  $5^\circ$  with displays having a strong haze component of reflection without substantial measurement error (less than 1 %). However, an incorrect source angle can produce large errors in the radiance-factor measurements for such displays. We thus limit the uncertainty of the  $\theta_s=45^\circ$  source angle to  $0.3^\circ$ . Future work will include establishing requisite apparatus uncertainties depending upon the reflection properties of the displays.

#### 4.2 Optimized-Sun Daylight Configuration

We have already laid the mathematical groundwork for this configuration in section 3.2. We can imagine a cell-phone user attempting to orient his transfective display in its reflective mode to be able to best read the information on the screen. To replicate such a condition we allow the display to be oriented in such a way to maximize contrast and/or readability (in the event the maximum contrast does not produce the best readability). The display may be observed anywhere from  $\theta_d \leq 30^\circ$  tilted away from the normal with the directed source simulating the sun oriented in some other direction for optimum viewing—see Fig. 3. In actual practice, the display is observed with the eye to establish the approximate best viewing configuration using the directed source, and then to optimize the results the measurements are made over a range of angles. Once the best orientation is established for contrast and/or readability, then the radiances are calculated for daylight conditions, as in Eq. (23), to provide the white screen spectral radiance  $K_W(\lambda)$  and the black screen spectral radiance  $K_K(\lambda)$

whereby the white and black luminances,  $K_w$  and  $K_k$ , under daylight conditions can be determined. Ideally, the source should have a subtense of  $\kappa_s = 0.5^\circ$ , but how much larger the source can be without jeopardizing the results is a matter for further research.

For the measurement of the radiance factor to be successful, reflections off the bezel and any other parts of the display must be carefully controlled so as to not affect the results because of veiling glare from bright surfaces other than the display. For most displays, it is unlikely that the best orientation will occur in a specular configuration ( $\phi_d = \phi_s \pm 180^\circ$ ). In general, such measurements are very sensitive to alignment and source configuration, particularly whenever the front surface has a nontrivial haze component of reflection and the observation direction is within  $30^\circ$  or less of the specular direction. For most displays at this optimum orientation, as the source subtense increases the contrast decreases; thus the small source specified can be advantageous. Because the optimum configuration is a property of the display and not a property of the exact angles employed, no uncertainty requirements need to be placed on the angles used for this configuration. A maximum in contrast (and readability) is sought after; we are not trying to obtain the contrast for a particular source-detector configuration with specified angles.

## 5 Experimental Results

The diffuse reflectance is measured with a sampling integrator. It is similar to a sampling integrating sphere, only this implementation has a pill-shaped rather than spherical interior (150 mm width, 225 mm length, 38 mm sample port diameter, and 30 mm measurement port diameter)—see Fig. 6. Sampling integrators are useful, for example, when the display is too large to be placed in available integrating spheres. Diffuse-reflectance measurements using this sampling integrator agree well within 1 % with results obtained by use of a large integrating sphere. A fiber-optic illuminator is used for the source of light inside the sampling integrator, which provides roughly 13 klx of illuminance with approximately the  $S_{\text{THIRB}}(\lambda)$  spectrum. Irradiance (illuminance) measurements are based upon the radiance (luminance) measurement of an interior wall patch near the sample port (not shown) with an assumed spectral reflectance of 0.99 (+0.002 / -0.005) over the visible spectrum. Unless otherwise stated, all the measurement results reported herein have an estimated 5 % (average, in the case of spectra) relative expanded uncertainty with a coverage factor of two.

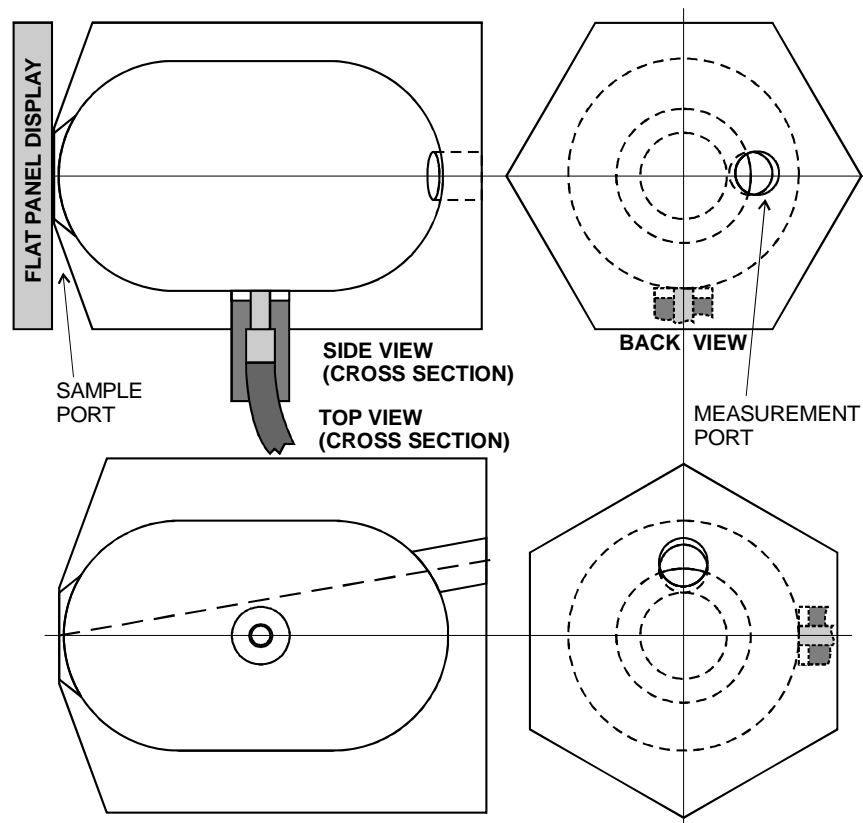


**Figure 6.** Sampling integrator providing a uniform diffuse illumination of the surface of the display. The sample port is placed next to the screen to be measured. The radiance and luminance measurements are made through the measurement port at  $10^\circ$  from the normal of the display and sample port. In practice, the sample port is placed just a fraction of a millimeter from touching the flat panel display to avoid any mechanical corruption of the measurement results.

### 5.1 Fixed-Sun Daylight Configuration

Spectral measurements are made with a spectroradiometer from 380 nm to 780 nm having a measurement field angle at infinity focus of  $\alpha = 0.25^\circ$  and an acceptance area diameter of 19.6 mm at a distance of  $c_d = 1.77$  m from the display. An eye with a 3 mm diameter pupil placed at 400 mm from the display subtends  $0.43^\circ$ . The lens of the spectroradiometer subtends  $0.63^\circ$  by comparison. We tested a liquid crystal display (LCD) with a microstructure front surface that produces primarily a haze component of reflection without a significant specular (distinct image) or Lambertian component. [10, 11] The spectral radiances of the screen from the normal direction are shown in Fig. 7. For the fixed-sun configuration with the source at  $45^\circ$ , the source subtends approximately  $3.5^\circ$  and produces approximately 20 klx of illumination also with the  $S_{\text{THRB}}(\lambda)$  spectrum. The spectral diffuse reflectance is shown in Fig. 8, and the spectral radiance factor is shown in Fig. 9. The luminances under daylight conditions are determined via Eqs. (33) and (24). The results are shown in Table 2. Whereas the screen exhibits a large

contrast ratio of  $J_W/J_K = 709$  in a darkroom, under daylight conditions the ambient contrast ratio is only  $D = 1.7$ . The reduction in contrast is largely from the contribution of the diffuse reflectance. If only a sun-level source were at  $45^\circ$  (no skylight,  $K_H$  with  $E_{\text{sky}} = 0$ ) then the contrast ratio would be 5:1. If only a bright sky were present (no direct sun,  $K_H$  with  $E_{\text{sun}} = 0$ ) then the contrast ratio would be 1.5:1. This is an example of why just pointing a sun-level source at a display and claiming sunlight readable is completely inadequate. The diffuse contribution is not ignorable.

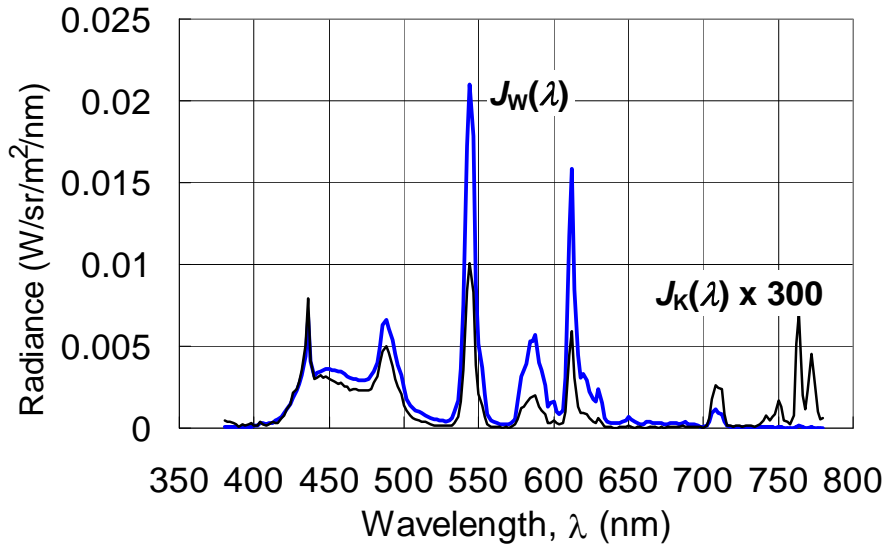


**Figure 7.** LCD darkroom radiances for white and black screens, where the black radiance has been amplified by a factor of 300 to render it visible on the same graph.

Table 2. Fixed-Sun Daylight Configuration				
$\rho_W = 0.0558$ $\rho_K = 0.0492$ $\beta_W = 0.00552$ $\beta_K = 0.00223$	Daylight Lumi- nance, $K_H$ (cd/m <sup>2</sup> )	Dark- room Lumi- nance, $J_H$ (cd/m <sup>2</sup> )	Calculated Contributions from Daylight	
			Skylight: $\rho_H E_{\text{sky}}/\pi$	Sunlight ( $\theta_s = 45^\circ$ ): $\beta_H E_{\text{sun}} \cos \theta_s/\pi$
White: H = W	1291	248	675	368
Black: H = K	749	0.350	626	123

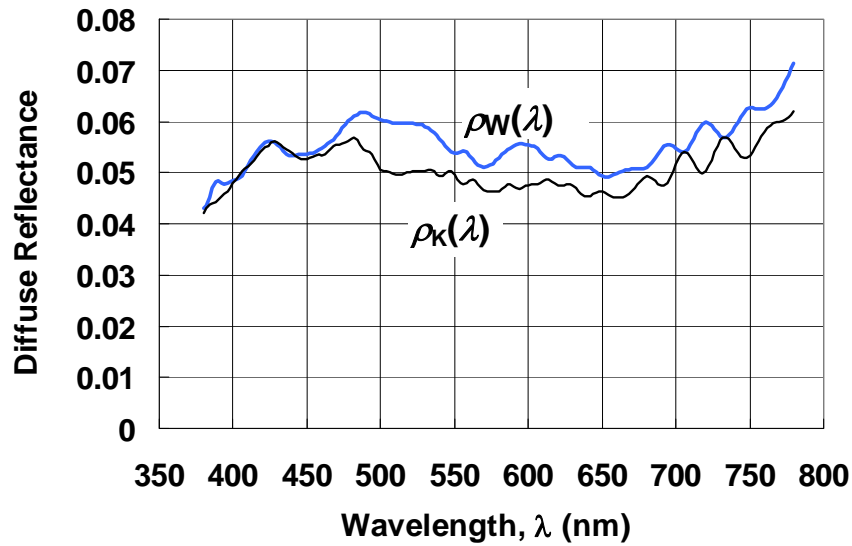


Figure 8. Spectral diffuse reflectance of a LCD.

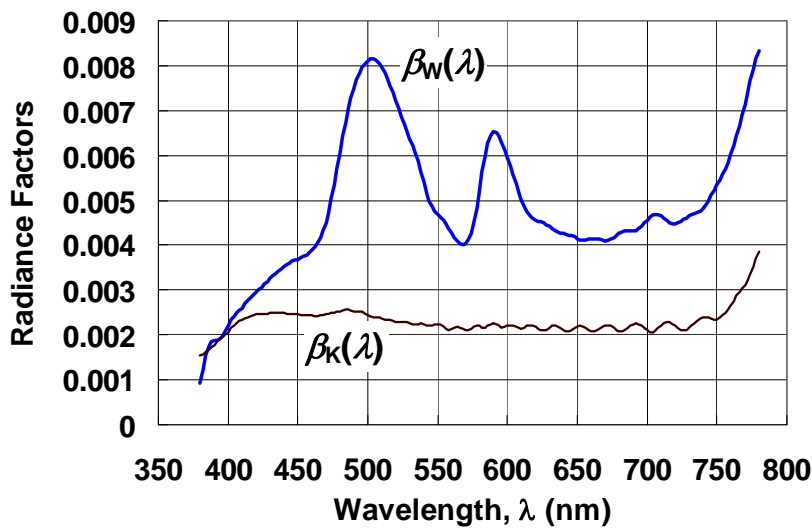


Figure 9. Spectral radiance factor of a LCD.

## 5.2 Optimized-Sun Daylight Configuration

A photopic measurement is made on a small cell-phone transfective display for the optimized-sun daylight configuration. (How successfully this may be compared to a full spectral measurement is discussed in the next section.) A luminance meter is used with measurement field angle at infinity focus of  $\alpha = 0.125^\circ$  and an acceptance area diameter of 19.6 mm at a distance of  $c_d = 1.20$  m from the display. The detector subtense is  $\kappa_d = 0.94^\circ$ . The fiber-optic source is placed at  $c_s = 400$  mm

and has a subtense of  $\kappa_s = 1.8^\circ$  in order to provide more light at the sacrifice of some contrast. (A source with a smaller subtense such as  $0.5^\circ$  would provide slightly more contrast.) By simply holding the display in sunlight and estimating the orientation that provides the best readability, the initial approximate angles for measurement are obtained. They are further refined by laboratory measurements: The source orientation employed for measurement is ( $\theta_s = 24^\circ$ ,  $\phi_s = 0$ ) and the detector is located at the normal of the display ( $\theta_d = 0$ ,  $\phi_d = 0$ ). We show the results of scanning the two source angles in Fig. 10. The results for the reflection parameters are found in Table 3. The ambient contrast ratio for full daylight conditions is  $D = 4.3$ . However, if no direct sunlight were to fall on the display on a bright day where the skylight illuminance is 10 000 lx ( $K_H$  with  $E_{\text{sun}} = 0$ ), the contrast ratio would be only 1.3:1. This is the contrast that would be observed if we obscured the direct sunlight falling on the display (as with our head when looking at a cell-phone display) and then tilting the display so that its normal pointed in a direction away from our head. Placing our head along the normal and obscuring the direct sunlight is an intermediate situation that will be addressed in a future paper. If the sky could somehow be eliminated ( $K_H$  with  $E_{\text{sky}} = 0$ ) the sun alone would produce a contrast ratio of 5.1:1.

Table 3. Optimized-Sun Daylight Configuration			
$\rho_W = 0.131$ $\rho_K = 0.099$ $\beta_W = 0.203$ $\beta_K = 0.040$	Daylight Luminance, $K_H$ (cd/m <sup>2</sup> )	Calculated Contributions from Daylight	
		Skylight: $\rho_H E_{\text{sky}}/\pi$	Sunlight ( $\theta_s = 24^\circ$ ): $\beta_H E_{\text{sun}} \cos \theta_s/\pi$
White: H = W	6331	416	5915
Black: H = K	1487	317	1171

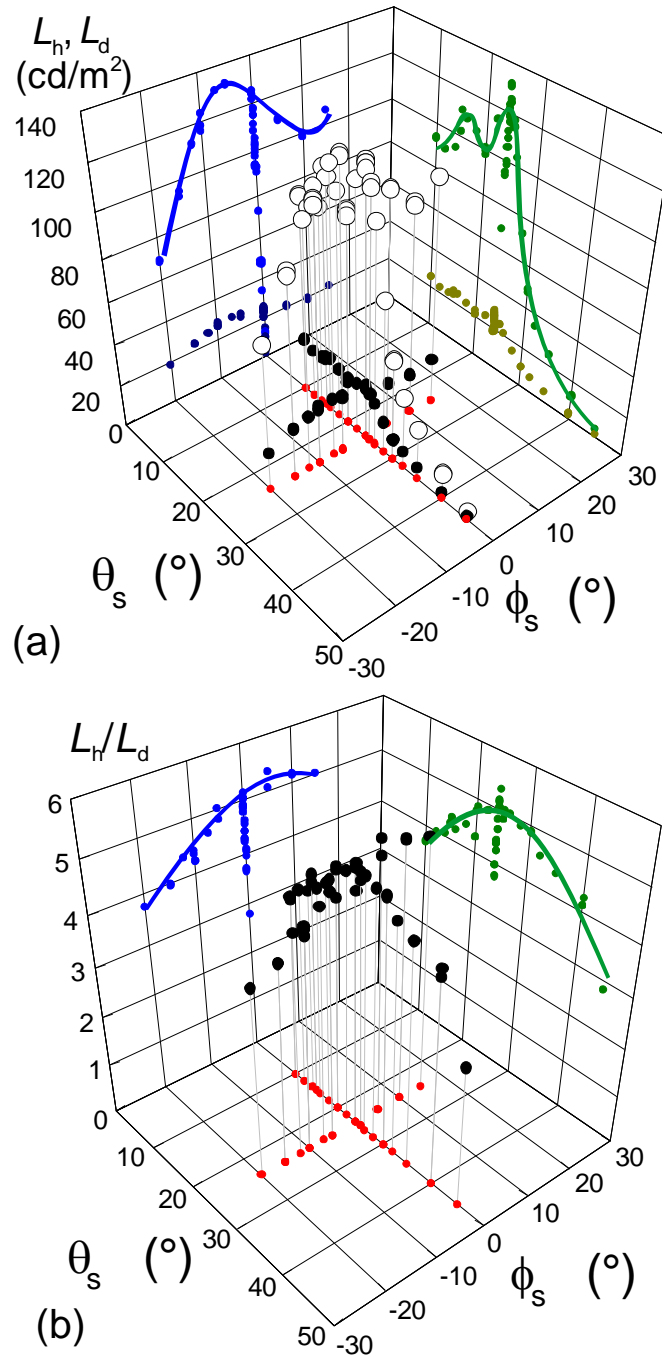


**Figure 10.** Luminance and contrast for the optimal-sun configuration of a transfective cell-phone display in its reflective mode in the vicinity of maximum readability. Plot (a) shows the luminances of white and black under directed illumination. Plot (b) shows the contrast ratio (without skylight). The solid lines are drawn by hand to indicate the shapes of the data. The contrast changes much less than the white luminance over the same range.

The comparison of the luminance data and the contrast in Fig. 10 reveals an important issue: Contrast is not the only important characteristic in making a display readable. The contrast changes rather slowly over the range of angles measured

compared to the dramatic change in white luminance over that same range. For example, at a sun angle of  $\theta_s = 40^\circ$  ( $\phi_s = 0$ ) the contrast is approximately 4:1—a reduction of 22 % from the maximum contrast—yet the luminance of white has decreased by a factor of 12, which would make the display virtually unreadable.

## 6 Photometric Measurement Concerns

We want to see how the irradiance spectrum affects the reflectance factor and diffuse reflectance for the LCD display under consideration. That is, for the LCD display, could we have simply made photopic measurements without regard to the illumination spectra as we did for the transfective display? It is interesting to compare the radiometric equations for the spectral radiances under daylight conditions, Eqs. (23) and (24), with their photopic equivalents expressed in Eq (25). We obtain expressions for the reflection parameters as found in Eq. (8) where  $R_H$  can be any of the photopic reflection parameters  $R_H = \beta_w, \beta_k, \rho_w,$  or  $\rho_k$  obtained from their spectral counterparts,  $R_H(\lambda) = \beta_w(\lambda), \beta_k(\lambda), \rho_w(\lambda),$  or  $\rho_k(\lambda)$ . Writing the irradiances using previously defined quantities  $f_D$  and  $G_D$  in Eqs. (4)–(6) we can write the reflection parameters as

$$R_H = \frac{\int V(\lambda)R_H(\lambda)S_D(\lambda)d\lambda}{G_D}, \quad (35)$$

where the values for  $G_D$  are found in Table 1. We can now employ different spectra  $S_D(\lambda)$  and calculate how the various photopic reflection parameters are affected by source spectra. The worst case situation occurs for the luminance factor for the white screen,  $\beta_w$ —the least gray reflection parameter. The white-screen radiance factor  $\beta_w(\lambda)$  is shown in Fig. 9 as the most nonuniform of all the display reflectance data obtained, and it is therefore the most sensitive to any nonuniformity in the illumination spectra. However, as shown in Table 4, the deviations in the resulting luminance factors are relatively small despite such remarkably different spectra from 16500 K skylight to 2856 K tungsten halogen. The mean luminance factor is 0.00549, the relative standard deviation is 2.4 %, and the maximum deviation is only 5.8 % between the tungsten-halogen source and the skylight source. This could suggest that the source spectrum for most broadband sources will not seriously affect the photopic measurement of the reflection parameters of gray-like displays if uncertainties of approximately 5 % up to 10 % are acceptable. However, such a recommendation cannot be followed with impunity, particularly when the display exhibits strong colors, or if colorimetric measurements are being made, or if the display exhibits a nontrivial fluorescence.

Table 4. Luminance Factor of White vs. Illumination Spectra					
Spectrum:	Tungsten Halogen	Tungsten Halogen with IR Blocking	Sunlight	Overcast Skylight	Skylight
(D):	(tung)	(THIRB)	(sun)	(over)	(sky)
CCT:	2856 K	3380 K	5500 K	6500 K	16 500 K
$\beta_w =$	0.00534	0.00538	0.00555	0.00552	0.00566

## 7 Readability Determination

Readability depends, in a complex way, on the contrast, the luminance, the character height, and the age of the reader. The perception of images is even more complex and beyond the scope of this paper. Models exist that can be applied for analysis of image quality in ambient lighting. [12, 13] For the purposes of this paper, we will define a simplified, approximate, step-by-step procedure suitable for use with daylight measurement methods. Other methods for determining readability may be found to be more useful. We present this as a possible mechanism to quantify the readability of a display rather than simply resorting to a measurement of contrast alone. For the purposes of this initial work, we will assume that the small-area or character stroke radiance (luminance) levels are the same as the full-screen levels for white and black. This is probably not very often the case for many displays. We are trying to develop the formalism here. Because of the difficulty in making accurate measurements of small dark areas on a white screen, we will confine our attention to full screen results and leave the small-area measurements under reflections for future research.

We employ the contrast definition that is used in the CIE 145 Visual Performance Model [14]:

$$C = |L_{ave} - L|/L_{ave} . \quad (36)$$

There are two cases to consider: positive polarity with black letters on a white background (the default case), and negative polarity with white letters on a black background. For the default case with black letters and a white background (positive polarity),  $L = K_K$  is the luminance of black with reflections included and  $L_{ave}$  is the local average luminance of the black text with a white background with reflections included [15]:

$$L_{ave} = 0.75K_W + 0.25K_K . \quad (37)$$

The contrast becomes

$$C = \frac{|0.75K_W - 0.75K_K|}{0.75K_W + 0.25K_K} = \frac{|K_W - K_K|}{K_W + (K_K/3)} . \quad (38)$$

In order to include the effects of luminance, character height and viewer age, we use the relative visual performance (RVP) model described in CIE 145. [14] The CIE RVP value  $P$  is between zero and one,  $0 \leq P \leq 1$ , where  $P = 1$  is normalized to the performance level of a young adult reading critical detail sizes of 4.5' (minutes of arc) with an average luminance of  $1000 \text{ cd/m}^2$ .  $P = 1$ , or 100 %, means that reading is 100 % accurate.

For our simplified case, we will employ a smaller text size than used to establish the CIE RVP value of 100 %. We fix the critical detail size to 1.5' of arc, which represents the size of stroke widths, diacritics, and punctuation of small font sizes common on many electronic displays (for a 400 mm viewing distance, a 1.5' mark would be 0.17 mm high and a typical character height might be 1.7 mm to 2.3 mm [15' to 20']). Using this critical detail size and the information in CIE 145, we can generate a family of curves for each age group. In Fig. 11 we show the curves for 20, 50 and 70-year-old adults. The RVP  $P$ -value is the ordinate, the curves are labeled according to the appropriate contrast, and the abscissa is the average luminance level.

	LCD	Transflective
$K_W \text{ (cd/m}^2\text{)}$	1291	6331
$K_K \text{ (cd/m}^2\text{)}$	749	1487
$D$	1.7	4.3
$L_{\text{ave}} \text{ (cd/m}^2\text{)}$	1156	5120
$C$	0.35	0.71
$P \text{ (20 y, 50 y, 75 y)}$	82 %, 67 %, 30 %	100 %, 87 %, 53 %

*Readability in positive polarity (black text on white):* First calculate the average luminance and contrast according to Eqs. (37) and (37). Then find the RVP value from the appropriate diagram for the luminance and the contrast for the appropriate age group. This procedure provides a simplified step-by-step way of calculating the readability in daylight ambient conditions. Readers needing more detailed predictions of the readability are advised to use the formulas published in CIE 145. These formulas enable predictions for a wide range of luminance levels, character sizes, and user ages. For example, suppose our daylight luminances are  $K_W = 800 \text{ cd/m}^2$  and  $K_K = 250 \text{ cd/m}^2$ ; then the average luminance is  $L_{\text{ave}} = 623 \text{ cd/m}^2$ , and the contrast is  $C = 0.62$ . For a 20-year old adult (discerning 1.5' detail), the RVP or readability is  $P = 0.95$ , or 95 %. To do the same thing using the graph for a 75-year old would result in a readability of  $P = 0.48$ , or 48 %.

For the displays measured above, the results are found in Table 5. The readability expressed in percent relative visual performance  $P$  for a 20-, 50-, and 75-year old is in the last row; it is based upon our example of the critical detail size at 1.5' of arc and obtained from Fig. 11. Compare the ambient contrast ratio  $D$  with the contrast  $C$  and the relative visual per-

formance  $P$ . The ambient contrast shows an improvement of 153 % between the LCD display and the transfective display, the contrast shows a 103 % improvement, and the relative visual performance shows an increase of 22 %, 30%, and 77 %, respectively.

*Readability in negative polarity (white text on black):* To roughly estimate the readability in negative polarity, multiply the RVP for the positive polarity with 0.9. This degradation value of 0.9 is an experience-based coefficient that is in line with published research. [16, 17]

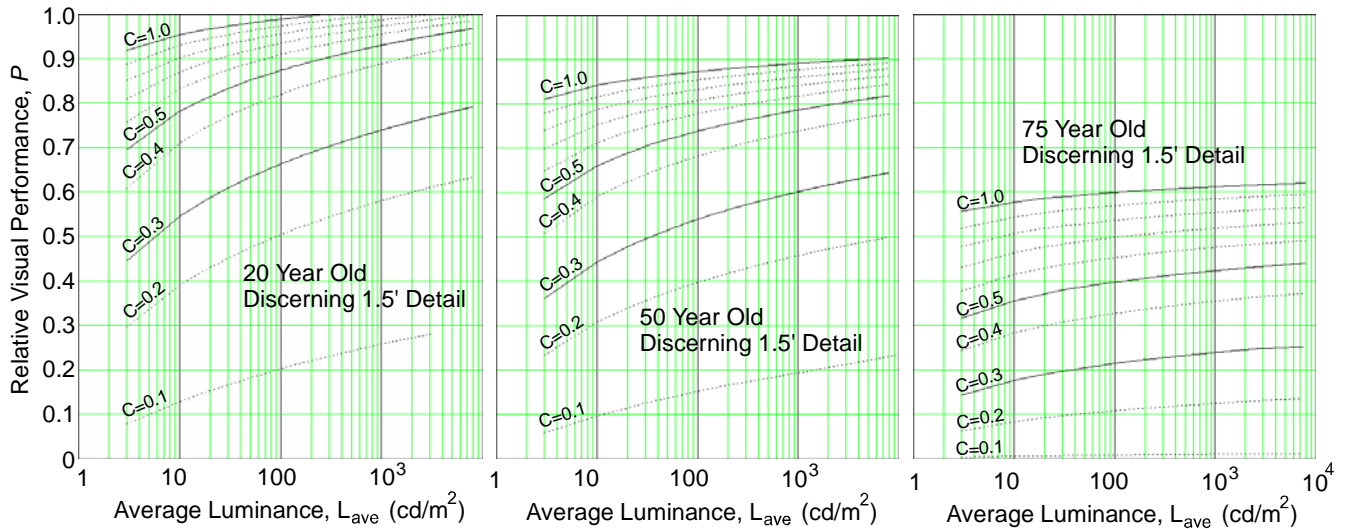


**Figure 11.** CIE RVP for 20-, 50-, and 75-year-old adults as a function of contrast and average luminance for the discernment of 1.5' of arc detail.

## 8 Conclusion

We have shown that realistic daylight measurements of displays involve not only direct sunlight, but also—and very importantly—a uniform diffuse contribution from skylight. Measurements of the reflection parameters are made using laboratory sources. Two directed-source configurations are presented, the fixed-sun and the optimized-sun configuration. Either can be combined with uniform diffuse illumination results and then scaled to daylight levels providing a measure of the ambient contrast for the display under daylight conditions. Combining these measurements with a vision model for detail discrimination provides a means of measuring display readability.

To avoid all the complications in attempting to produce the correct illumination CCT, it is our initial recommendation that these measurements be made spectrally and then the appropriate skylight or sunlight spectra be used to determine the performance of the display under daylight conditions. If only photometric measurements are to be made without attention

to the correct spectra for the daylight illuminants, then errors in the reflection parameters values of approximately 5 % or more might be anticipated when compared with spectrally resolved measurement results.

In making any of these measurements there are several important matters to keep in mind in order to accurately measure the reflection parameters:

1. **Avoid Heat:** Avoid heating the display with the illumination as much as possible. Some displays exhibit a dramatic temperature dependence. If the source can heat the display, a shutter (or equivalent) can usually be employed so that the display is exposed to the source only during the measurements. If a sampling sphere is used and may heat the display, it can usually be backed away from the display to avoid heating without having to turn off the lamp.
2. **Bright Source:** For emissive displays, arrange for the illuminating source to provide sufficient light so that the reflected spectral radiance (luminance) is sufficiently large to be measured above the emissive spectral radiance (luminance) of the display showing white. This is necessary because of the subtraction to get the net reflected spectral radiance (luminance)—see Eq. (11).
3. **Same Place:** The subtracted spectral radiance (luminance) measurements of an emissive display in a darkroom and under illumination must be measured at exactly the same place on the screen because of screen luminance nonuniform.
4. **Same Angle:** The subtracted spectral radiance (luminance) measurements of an emissive display in a darkroom and under illumination must be made at the same angle because of the possible viewing angle dependence of the screen.
5. **Same Time:** The spectral radiance (luminance) measurements need to be made at approximately the same time because of the possibility of the screen changing its characteristics with time.

Future work will focus on several features: (1) We intend to further investigate the requirements of the source subtense for the directed source in both measurement apparatus configurations to better identify the permissible ranges. (2) The importance of the full-spectral measurement for a large variety of displays needs to be investigated. Also, color measurements under reflection need to be carefully considered. (3) There are certain conditions where a filter can be put in front of the detector to simulate the daylight spectra results, but more work is needed to define and understand these conditions. (4) If displays exhibit fluorescence, methods need to be developed to guide their characterization. (5) Finally, a new configuration is under investigation that simulates the user's head obscuring some of the bright surround—a configuration that simulates a person using a cell phone under daylight conditions.

## References

1. G. Wyszecki and W.S. Stiles, “Color Science: Concepts and Methods, Quantitative Data and Formulae,” 2nd Ed., 2000, John Wiley & Sons, New York, p. 4-11, 28, 146, 762.

2. CIE 15:2004, *Colorimetry*, 3rd edition, Commission Internationale de l'Eclairage (International Commission on Illumination), CIE Central Bureau, Vienna, Austria, 2004.
3. The CIE does not define the "luminous reflectance factor." We introduce the adjective "luminous" to distinguish it from its radiometric counterpart—private communications with Dr. Yoshi Ohno, NIST.
4. CIE Publication No. 17.4, *International Lighting Vocabulary*, Commission Internationale de l'Eclairage (International Commission on Illumination), 1987. A joint publication with the International Electrotechnical Commission: IEC Publication 50(845), *International Electrotechnical Vocabulary*, Chapter 845: Lighting, 1987.
5. CIE Publication No. 69, *Methods of Characterizing Illuminance and Luminance Meters*, Commission Internationale de l'Eclairage (International Commission on Illumination), 1987.
6. CIE Publication No. 44, *Absolute Methods for Reflection Measurement*, Commission Internationale de l'Eclairage (International Commission on Illumination), 1979 reprinted 1990.
7. Y. Ohno, "CIE Fundamentals for Color Measurements," IS&T NIP16 Conference, Vancouver, Canada, Oct. 16-20, 2000.
8. S. Nevas, F. Manoocheri, and E. Ikonen, "Gonioreflectometer for Measuring Spectral Diffuse Reflectance," *Applied Optics*, Vol. 43, No. 35, pp. 6391-6399, 10 Dec. 2004.
9. E. F. Kelley and J. Penczek, "Scalability of OLED Fluorescence in Consideration of Sunlight-Readability Reflection Measurements," 2004-SID International Symposium Digest of Technical Papers, Society for Information Display, Paper P.54, Vol. 35, Book 1, pp. 450-453, Seattle, WA, May 25, 2004.
10. E. F. Kelley, G. R. Jones, and T. A. Germer, "Display Reflectance Model Based on the BRDF," *Displays*, Vol. 19, No. 1, pp. 27-34, June 30, 1998.
11. E. F. Kelley, G. R. Jones, and T. A. Germer, "The Three Components of Reflection," *Information Display*, Vol. 14, No. 10, pp. 24-29, October 1998.
12. P. Barten, "Formula for the contrast sensitivity of the human eye," *Image Quality and System Performance*, San Jose, California, pp. 231-238, January 18, 2004; ISBN / ISSN: 0-8194-5197-5.
13. L. Silverstein, et al., "Effects of spatial sampling and luminance quantization on the image quality of color matrix displays," *J. Opt. Soc. Am. A*, Vol. 7, No. 10, 1990.
14. CIE 145:2002, *The Correlation of Models for Vision and Visual Performance*, Commission Internationale de l'Eclairage (International Commission on Illumination), CIE Central Bureau, Vienna, Austria, 2002.
15. I. Baily, R. Clear, and S. Berman "Size as a Determinant of Reading Speed," *J. Illum. Eng. Soc.*, Vol. 22, No. 2, pp. 102-113, 1993.

16. L. V. Scharff and A. J. Ahumada, "Understanding Text Polarity Effects," ECVP (European Conference on Visual Perception), A Coruña, Spain, Aug. 2005.
17. T. Mustonen and M. Lindfors, "Pixel Defects on a Small High-Density Display – Effects on Visual Performance and Perceived Quality," SID EuroDisplay, Edinburgh, Scotland, Sep. 2005.